Magnetic Levitation System: Analysis & Control

ENGR 6131: Term Project

Instructor: Dr. Kash Khorasani

Department of Electrical and Computer Engineering, Concordia University

Braden Stefanuk (40137204)
Parthkumar Viradiya (40125453)

December 18, 2019

Abstract

With the large number of unique methods that can be used control any given dynamic system, it is often difficult for elementary practitioners to know which method is the most appropriate for a specific system. Classical control and modern control techniques often provide alternative and, in some sense, mutually exclusive advantages. In this work a magnetic levitation system is modelled, analyzed, and controlled using a PID controller and a full state feedback controller. The closed loop response of both methods are plotted for a number of input signals, and the methodology followed to achieve such controllers is worked in detail. Their relative advantages are illuminated by comparing each controller against a set of predefined design specifications. Furthermore, the process of constructing each controller is discussed and analyzed in the context of the specific magnetic levitation system used. Through the work done in this report the reader will gain a deeper understanding of general design considerations for higher order dynamic systems, and will build an intuition for the pros and cons of classical and modern control techniques. In the end, it was concluded that full state feedback is a preferable approach to control the dynamics of the magnetic levitation system.

Contents

1 Introduction

The field of control systems is deep, and has many routes within it that allow the control engineer a considerable amount of leniency in the design process. For over a century now, the method of Proportional Integral Derivative (PID) control has been established, finding success in many industries to this day. Other techniques, such as lead and lag control, use analysis and design techniques similar to PID. These techniques constitute a class of control theory called Classical Control; generally speaking, these techniques map the input of a system to its output by modelling the dynamics of the system in terms of a *transfer function*.

Prompted largely by the need for highly sophisticated control techniques in military and space applications, the field now known as Modern Control began to emerge in the mid 1900s as another option for control engineers. Modern Control is predicated on the concept of the state, starkly different from that of Classical Control, which is concerned primarily with the relationship between a system's output and input. Concepts such as *state space*, *controllability*, *observability*, and *state estimation* belong to the school of Modern Control. Although it is considered to be more mathematically involved, this theory provides insights, capabilities, and precision unavailable to classical methods.

In this work, a magnetic levitation system (Fig. 1) will be simulated, analyzed, and controlled from both a classical and modern perspective. By the end of this report, a selection will be made addressing which of the two control techniques, PID or full state feedback, is preferrable for the magnetic levitation device in Fig. 1. The report is organized as follows. In Section 2 we summarize the problem that we aim to address followed by an outline of the self-imposed design specifications in Section 3. Section 4 covers the process of linearizing the equations of motion, evaluating the transfer matrix governing the system, computing the state and output equations, as well as the MATLAB functions and workflow used to realize the control systems presented. In Section 5 the responses of the control systems to various input signals are graphically visualized and analyzed with respect to the proposed specifications. Section 6 contains a comparative discussion relating the advantages and disadvantages of the methods explored, as well as any road-blocks of that were encountered along the process of implementing them. Section 7 concludes the report and highlights lessons learned and recommendations for the future.

2 Problem Statement

The problem that this work aims to solve is as follows:

> For the magnetic levitation apparatus shown in Fig. 2, is it preferable to employ Proportional Integral Derivative or Full-State-Feedback to control the position of the magnets?

Two distinct metrics will be used to assess the outcome of the above question, these metrics are:

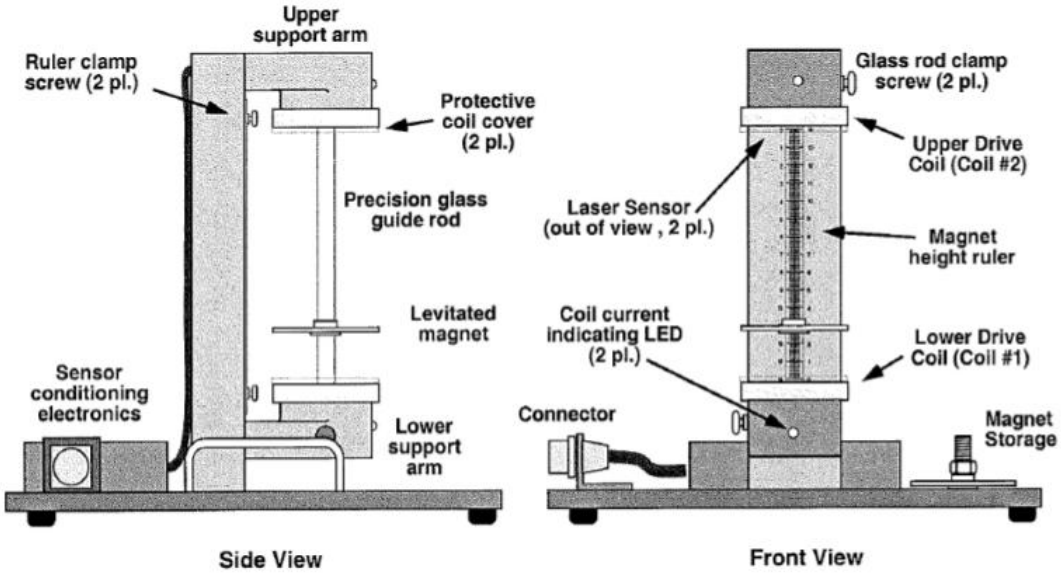

Figure 1: Overview of the magnetic levitation apparatus being modelled (image retrieved from project description).

1. The ability of the control method to feasibly meet the proposed design specifications.
2. The ease of implementing and optimizing the control method such that the design specifications are met as closely as possible.

3 Design Specifications

Since all of our control parameter testing will be conducted in the time domain, it makes sense to define design specifications in the time domain as well. The specifications we have chosen for our system are: maximum overshoot y_{max}; rise time t_r, that is, the time it takes for the system to rise from 10% to 90% of the steady state position; and settling time t_s. The values of these specifications are given in Table 1. It is important to note that for the settling time a tolerance of 2% of the steady state value has been chosen.

Specification	Value
Peak overshoot (y_{max})	$<$ 2 mm ($<$ 10%)
Rise time (t_r)	$<$ 5 s
Settling time (t_s)	$<$ 10 s

Table 1: Design specifications for the magnetic levitation system

4 Methodology

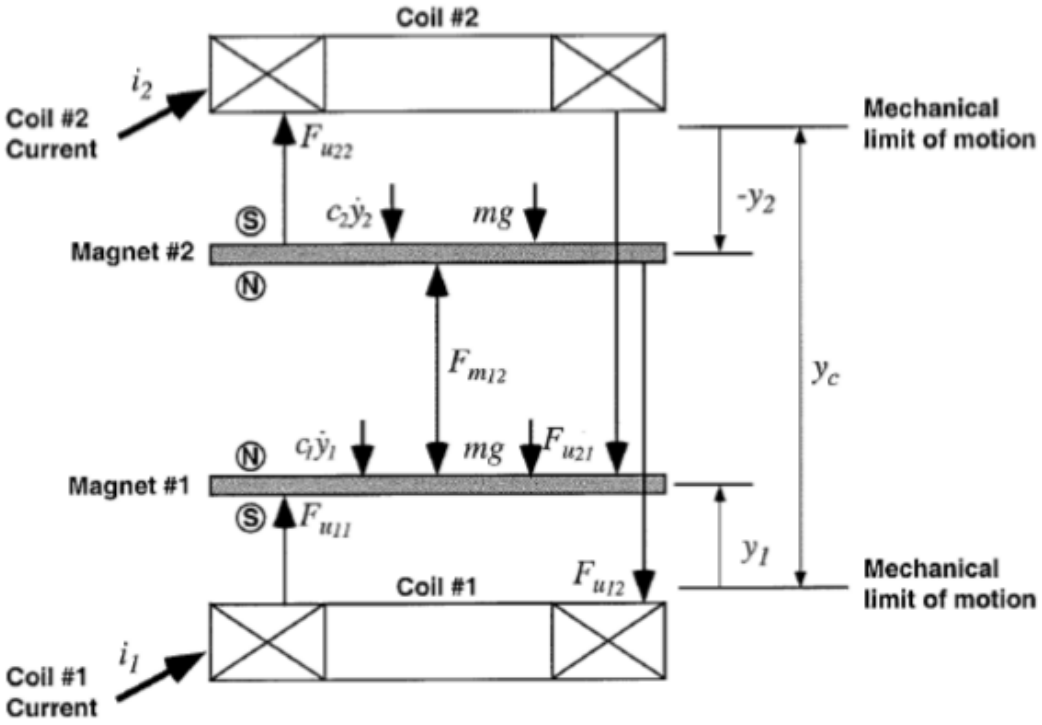

Figure 2: Free body diagram for the double magnet apparatus being modelled (image retrieved from project description).

We begin our exploration of the control and analysis of the MagLev apparatus shown in Fig. 2 with the full order nonlinear model:

$$m\ddot{y}_1 + c_1\dot{y}_1 + F_{m_{12}} = F_{u_{11}} - F_{u_{21}} - mg \tag{1}$$
$$m\ddot{y}_2 + c_2\dot{y}_2 - F_{m_{12}} = F_{u_{22}} - F_{u_{12}} - mg. \tag{2}$$

This model can be simplified considerably by assuming that the force imparted on each magnet from the distant coil is negigible compared to the force imparted by the closer coil. Furthermore, given that the MegLav apparatus is intended to be employed in air, we will assume that the drag forces (velocity dependent forces) are also negligible. Together this implies that we can set the terms $F_{u_{12}} = F_{u_{21}} = c_1\dot{y}_1 = c_2\dot{y}_2 = 0$ and still retain the integrity of our model. The simplified equations of motion can be written as:

$$m\ddot{y}_1 = F_{u_{11}} - F_{m_{12}} - mg \tag{3}$$
$$m\ddot{y}_2 = F_{u_{22}} + F_{m_{12}} - mg, \tag{4}$$

where we can approximate the magnetic forces by the equations,

$$F_{u_{11}} = \frac{u_1}{a(y_1 + b)^N} \qquad F_{u_{22}} = \frac{u_2}{a(-y_2 + b)^N} \qquad F_{m_{12}} = \frac{c}{(y_{12} + d)^N}. \tag{5}$$

In Eq. 5 the factors u_1 and u_2 denote the current running through coil 1 and 2, respectively; the constants a, b, c, d, N are model parameters that have been selected to be,

$$a = 1.65 \qquad b = 6.20 \qquad c = 2.69 \qquad d = 4.20 \qquad N = 4. \tag{6}$$

For the purpose of notation, only $N = 4$ will be substituted into the magnetic force equations unless otherwise specified.

4.1 Linearization

Now, evidenced by the fourth order polynomial in the denominator of Eq. 5, the forces are not linear in y_1 or y_2, . Although this presents a formidable obstacle with regard to modelling the control structure of the system, we can approximate Eqs. 3, 4 by expanding them in a Taylor series. Since a Taylor series expansion will only approximate the accelerations $\ddot{y}_1$, $\ddot{y}_2$ evaluated at certain points, we select the operating conditions:

$$y_{1,o} = 2.00\text{cm} \qquad y_{2,o} = -2.00\text{cm} \tag{7}$$

And we will define the use the geometry and properties of the device to define $y_c = 12.0$cm and $m = 0.120$kg. Although the intended operating positions of either magnet are known, the amount of current in coil 1 and coil 2 required to maintain these operating positions are unknown. With Eq. 3, 4, we can use Newton's second law to solve for u_1 and u_2 by noting that at the operating point there should be no motion of either magnet, that is $\ddot{y}_1 = \ddot{y}_2 = 0$. Hence we have the equations, at the operating point,

$$0 = \frac{u_1}{a(y_1 + b)^4} - \frac{c}{(y_c + y_2 - y_1 + d)^4} - mg \tag{8}$$

$$0 = \frac{u_2}{a(-y_2 + b)^4} + \frac{c}{(y_c + y_2 - y_1 + d)^4} - mg. \tag{9}$$

Solving for the currents u_1 and u_2 respectively,

$$u_1 = a(y_1 + b)^4 \left(\frac{c}{(y_c + y_2 - y_1 + d)^4} + mg \right) \tag{10}$$

$$u_2 = a(-y_2 + b)^4 \left(-\frac{c}{(y_c + y_2 - y_1 + d)^4} + mg \right) \tag{11}$$

Substituting in values from Eqs. 6, 7, we find that the operating currents are,

$$u_{1,o} = 2927.14\text{A} \tag{12}$$

$$u_{2,o} = 2887.54\text{A} \tag{13}$$

Expanding in a Taylor series about $y_{1,o}$, $y_{2,o}, u_{1,o}$, and $u_{2,o}$ and truncating to first order,

$$m\ddot{y}_1 \approx -\left(\frac{4u_{1,o}}{ay_a^5} + \frac{4c}{y_d^5}\right)(y_1 - y_{1,o}) + \frac{4c}{y_d^5}(y_2 - y_{2,o}) + \frac{1}{ay_a^4}(u_1 - u_{1,o}) \tag{14}$$

$$\approx -\left(\frac{4u_{1,o}}{ay_a^5} + \frac{4c}{y_d^5}\right) y_1' + \frac{4c}{y_d^5} y_2' + \frac{1}{ay_a^4} u_1' \tag{15}$$

$$m\ddot{y}_2 \approx \frac{4c}{y_d^5}(y_1 - y_{1,o}) + \left(\frac{4u_{2,o}}{ay_b^5} - \frac{4c}{y_d^5}\right)(y_2 - y_{2,o}) + \frac{1}{ay_b^4}(u_2 - u_{2,o}) \tag{16}$$

$$\approx \frac{4c}{y_d^5} y_1' + \left(\frac{4u_{2,o}}{ay_b^5} - \frac{4c}{y_d^5}\right) y_2' + \frac{1}{ay_b^4} u_2' \tag{17}$$

where we have set $y_a = (y_{1,o} + b)$, $y_b = (-y_{2,o} + b)$ and $y_d = (y_{12,o} + d)$, and replaced $(y_i - y_{i,o}) = y_i'$ and $(u_i - u_{i,o}) = u_i'$. Also note that the zeroth order terms vanish since we are evaluating at the operating point. As complicated as it may look this is indeed a linear system in the variables y_1', y_2', u_1' and u_2'.

4.2 State Space Representation and the Transfer Matrix

Noting that our system evolves according to two second order differential equations, indicating that our problem is of fourth order, let us define the state vector $\boldsymbol{x} \in \mathbb{R}^4$ as the vector,

$$\boldsymbol{x} = [x_1\ x_2\ x_3\ x_4]^T, \tag{18}$$

where the variables x_i, $i = 1, 2, 3, 4$, are the state variables. With reference to Eq. 3, 4 we select the state variables,

$$x_1 = y_1' \qquad x_2 = y_2' \qquad x_3 = \dot{y}_1' \qquad x_4 = \dot{y}_2'. \tag{19}$$

and their time derivatives,

$$\dot{x}_1 = \dot{y}_1' \qquad \dot{x}_2 = \dot{y}_2' \qquad \dot{x}_3 = \ddot{y}_1' \qquad \dot{x}_4 = \ddot{y}_2'. \tag{20}$$

It is easy to see that by defining x_3, x_4 as the time derivatives of x_1, x_2, we have $\dot{x}_1 = x_3$ and $\dot{x}_2 = x_4$. To write $\dot{x}_3$, $\dot{x}_4$ in terms of state variables, we can use the linear approximation in Eqs. 15, 17, which can be parametrized in terms of x_1, x_2,

$$\dot{x}_1 = x_3, \tag{21}$$

$$\dot{x}_2 = x_4, \tag{22}$$

$$\dot{x}_3 = -\frac{1}{m}\left(\frac{4u_{1,o}}{ay_a^5} + \frac{4c}{y_d^5}\right)x_1 + \frac{4c}{my_d^5}x_2 + \frac{1}{may_a^4}u_1, \tag{23}$$

$$\dot{x}_4 = \frac{4c}{my_d^5}x_1 + \frac{1}{m}\left(\frac{4u_{2,o}}{ay_b^5} - \frac{4c}{y_d^5}\right)x_2 + \frac{1}{may_b^4}u_2. \tag{24}$$

In this way, our state equation can be written in matrix form as,

$$\begin{bmatrix}\dot{x}_1\\ \dot{x}_2\\ \dot{x}_3\\ \dot{x}_4\end{bmatrix} = \underbrace{\begin{bmatrix} 0 & 0 & 1 & 0\\ 0 & 0 & 0 & 1\\ -\frac{1}{m}\left(\frac{4u_{1,o}}{ay_a^5} + \frac{4c}{y_d^5}\right) & \frac{4c}{my_d^5} & 0 & 0\\ \frac{4c}{my_d^5} & \frac{1}{m}\left(\frac{4u_{2,o}}{ay_b^5} - \frac{4c}{y_d^5}\right) & 0 & 0\end{bmatrix}}_{A}\begin{bmatrix}x_1\\ x_2\\ x_3\\ x_4\end{bmatrix} + \underbrace{\begin{bmatrix} 0 & 0\\ 0 & 0\\ \frac{1}{may_a^4} & 0\\ 0 & \frac{1}{may_b^4}\end{bmatrix}}_{B}\begin{bmatrix}u_1'\\ u_2'\end{bmatrix} \tag{25}$$

with corresponding output equation,

$$\begin{bmatrix}w_1\\ w_2\end{bmatrix} = \begin{bmatrix}1 & 0 & 0 & 0\\ 0 & 1 & 0 & 0\end{bmatrix}\begin{bmatrix}x_1\\ x_2\\ x_3\\ x_4\end{bmatrix} + \mathbf{0}_{2\times 2}\begin{bmatrix}u_1'\\ u_2'\end{bmatrix} \tag{26}$$

where w_1, w_2 are used as output variables to avoid confusion with the initial position variables used earlier in the report.

If we define the matrices for the output as C and D, then evaluating A and B at their relevant parameter vales we get the quadruple,

$$A = \begin{bmatrix} 0 & 0 & 1 & 0\\ 0 & 0 & 0 & 1\\ -6.414 & 0.06243 & 0 & 0\\ 0.06243 & 6.203 & 0 & 0\end{bmatrix} \quad B = 3.374\text{e}{-3}\begin{bmatrix}0 & 0\\ 0 & 0\\ 1 & 0\\ 0 & 1\end{bmatrix} \quad C = \begin{bmatrix}1 & 0 & 0 & 0\\ 0 & 1 & 0 & 0\end{bmatrix} \quad D = \mathbf{0}_{2\times 2}. \tag{27}$$

We can compute the transfer matrix using the equation $H(s) = C(s\boldsymbol{I} - A)^{-1}B + D$, but given the human effort required to invert a 4×4 matrix it is more prudent to compute it in MATLAB

(see Appendix A). For the relation Y(s) = H(s)U(s) we receive the entries,

$$H_{11} = \frac{(3.374\text{e}{-3})s^2 - 0.02093}{s^4 + 0.2108s^2 - 39.79} \tag{28}$$

$$H_{12} = H_{21} = 0 \tag{29}$$

$$H_{22} = \frac{(3.374\text{e}{-3})s^2 + 0.02164}{s^4 + 0.2108s^2 - 39.79} \tag{30}$$

At this juncture it is important to note that the off-diagonal terms of $H(s)$, that is, H_{12}, H_{21} will be ignored such that our system represents two decoupled single-input single-output (SISO) systems. The transfer functions that govern the input-ouput relationship of these SISO systems are given by H_{11} and H_{22}, respectively.

4.3 Computation of the Canonical Forms

Beginning with the state space representation of Eq. 27, we can transform this quadruple into the Observable Canonical Form (OCF), Controllable Canonical Form (CCF), and Jordan Canonical Form (JCF). Before doing this however, it should be noted that, as per the decoupling above, we will receive two sets of quadruples, one for each of the two SISO systems.

The OCF and CCF for both SISO systems were evaluated routinely by analyzing the coefficients in the transfer functions of Eq. 28 and 30, and using standard formulas for the respective forms. Furthermore, the JCF was computed using a partial fraction expansion of the same transfer functions. Since there were no repeated poles, the JCF could be constructed by analyzing the expanded transfer functions and applying the formulas given in the lecture notes (Slide 37). The values in each of these canonical forms were verified in MATLAB using the functions `canon` and `jordan` (see lines 52 and 62 of `model.m` in Appendix A). Results of the canonical forms are given in Section 5.

4.4 Design of the Controllers and Observers

The development and design of the controllers and observers presented in the following sections were done in MATLAB. Standard MATLAB functions were used, as well as a few tool-kits and extensions for control system design. Given that the inputs and outputs were decoupled, as mentioned in the preceeding text, controllers were designed for each system seperately. The scripts `PID_1.m` and `PID_4.m` contain end-to-end control implementation and visualization for the two systems, respectively. This format is shadowed by the scripts `FSFB_1.m` and `FSFB_4.m`, which contain all of the code relevant to the full state feedback controllers and plots. Similarly, the full order observers are constructed in `FOO_1.m` and `FOO_4.m`, while their reduced order variants are contstructed in `ROO_1.m` and `ROO_4.m`. For the reduced order observers, it was assumed that state 1 is available and thus states 2,3, and 4 were estimated for both systems. All of the code used for

this report is included in Appendix A.

5 Results & Analysis

This section includes the relevant results and plots of both control system for the specific tasks outlined in the Project Description.

5.1 State Equations, Transfer Functions, and Canonical Forms

For simplicity, the system with input u_1 and output y_1 has been named **system-1** and the system with input u_2 and output y_2 has been named **system-2**. To begin, the original MIMO state space representation is shown again, along with the factored transfer functions for each decoupled SISO system.

State and output equations:

$$A = \begin{bmatrix} 0 & 0 & 1 & 0 \\ 0 & 0 & 0 & 1 \\ -6.414 & 0.06243 & 0 & 0 \\ 0.06243 & 6.203 & 0 & 0 \end{bmatrix} \quad B = 3.374\text{e}{-3} \begin{bmatrix} 0 & 0 \\ 0 & 0 \\ 1 & 0 \\ 0 & 1 \end{bmatrix} \quad C = \begin{bmatrix} 1 & 0 & 0 & 0 \\ 0 & 1 & 0 & 0 \end{bmatrix} \quad D = \mathbf{0}_{2\times 2}. \tag{31}$$

Transfer functions:

$$H_1(s) = \frac{(3.374\text{e}{-3})s^2 - 0.02093}{s^4 + 0.2108s^2 - 39.79} \tag{32}$$

$$= \frac{0.003374(s - 2.491)(s + 2.491)}{(s - 2.491)(s + 2.491)(s^2 + 6.414)} \tag{33}$$

$$H_2(s) = \frac{(3.374\text{e}{-3})s^2 + 0.02164}{s^4 + 0.2108s^2 - 39.79} \tag{34}$$

$$= \frac{0.0033742(s^2 + 6.414)}{(s - 2.491)(s + 2.491)(s^2 + 6.414)} \tag{35}$$

The transfer functions of the open-loop systems as in Eq. 33 and 35 have been factored to show the pole-zero locations more clearly. The associated canonical forms for system-1 and system-2 follow as:

Canoncial forms for system-1:

$$A_{O,1} = \begin{bmatrix} 0 & 0 & 1 & 39.79 \\ 1 & 0 & 0 & 0 \\ 0 & 1 & 0 & -0.2108 \\ 0 & 0 & 1 & 0 \end{bmatrix} \quad B_{O,1} = \begin{bmatrix} 1 \\ 0 \\ 0 \\ 0 \end{bmatrix}$$

$$C_{O,1} = [0 \quad 3.374\text{e}{-3} \quad 0 \quad -0.02164] \quad D_{O,1} = 0$$

$$A_{C,1} = \begin{bmatrix} 0 & 1 & 0 & 0 \\ 0 & 0 & 1 & 0 \\ 0 & 0 & 0 & 1 \\ 39.79 & 0 & -0.2108 & 0 \end{bmatrix} \quad B_{C,1} = \begin{bmatrix} 0 \\ 3.374\text{e}{-3} \\ 0 \\ -0.02164 \end{bmatrix}$$

$$C_{C,1} = [1 \quad 0 \quad 0 \quad 0] \quad D_{C,1} = 0$$

$$A_{J,1} = \begin{bmatrix} -2.491 & 0 & 0 & 0 \\ 0 & 2.491 & 0 & 0 \\ 0 & 0 & -j2.533 & 0 \\ 0 & 0 & 0 & j2.533 \end{bmatrix} \quad B_{J,1} = \begin{bmatrix} 1 \\ 1 \\ 1 \\ 1 \end{bmatrix}$$

$$C_{J,1} = [0 \quad 0 \quad j6.661\text{e}{-4} \quad -j6.661\text{e}{-4}] \quad D_{J,1} = 0$$

Canoncial forms for system-2:

$$A_{O,2} = \begin{bmatrix} 0 & 0 & 1 & 39.79 \\ 1 & 0 & 0 & 0 \\ 0 & 1 & 0 & -0.2108 \\ 0 & 0 & 1 & 0 \end{bmatrix} \quad B_{O,2} = \begin{bmatrix} 1 \\ 0 \\ 0 \\ 0 \end{bmatrix}$$

$$C_{O,2} = [0 \quad 3.374\text{e}{-3} \quad 0 \quad 0.02093] \quad D_{O,2} = 0$$

$$A_{C,2} = \begin{bmatrix} 0 & 1 & 0 & 0 \\ 0 & 0 & 1 & 0 \\ 0 & 0 & 0 & 1 \\ 0 & 0 & -0.2108 & 0 \end{bmatrix} \quad B_{C,2} = \begin{bmatrix} 0 \\ 3.374\text{e}{-3} \\ 0 \\ 0.02093 \end{bmatrix}$$

$$C_{C,1} = [1 \quad 0 \quad 0 \quad 0] \quad D_{C,1} = 0$$

$$A_{J,2} = \begin{bmatrix} -2.491 & 0 & 0 & 0 \\ 0 & 2.491 & 0 & 0 \\ 0 & 0 & -j2.533 & 0 \\ 0 & 0 & 0 & j2.533 \end{bmatrix} \quad B_{J,2} = \begin{bmatrix} 1 \\ 1 \\ 1 \\ 1 \end{bmatrix}$$

$$C_{J,2} = [-0.6773\text{e}{-4} \quad 6.773\text{e}{-4} \quad 0 \quad 0] \quad D_{J,2} = 0$$

5.2 Open-loop Responses and Characteristics

The open-loop impulse and step response of system-1 is displayed in Fig. 3 while the impulse and step response of system-2 are shown in Fig. 4. From these figures it is evident that both of the uncompensated systems unstable. This assessment if further verified by Fig. 5 and 6, where it it can be seen in the root locus plot that both systems have two poles on ths imaginary axis, and two real poles, one of which lies in the right-half plane. As a consequence, the open-loop system 2 is highly unstable since the two imaginary poles contribute to undamped oscillation

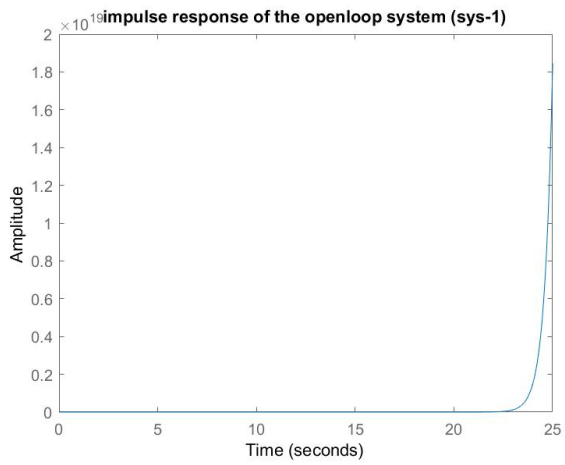

(a)

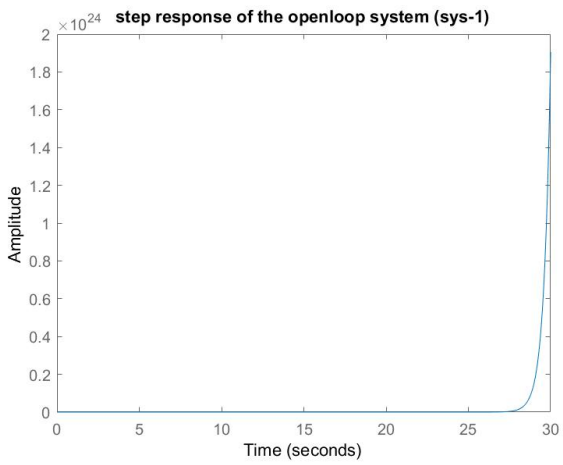

(b)

Figure 3: Open-loop impulse response (a) and step response (b) of **system-1**.

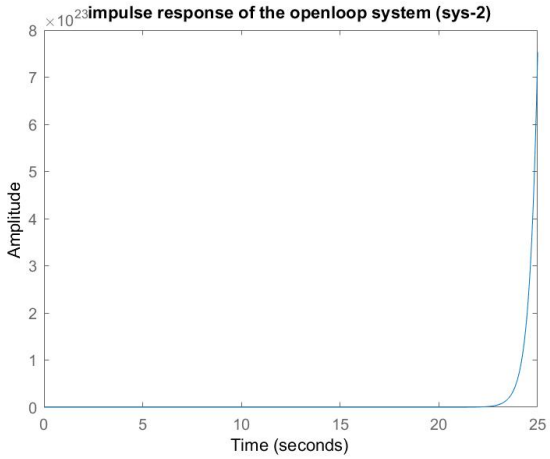

(a)

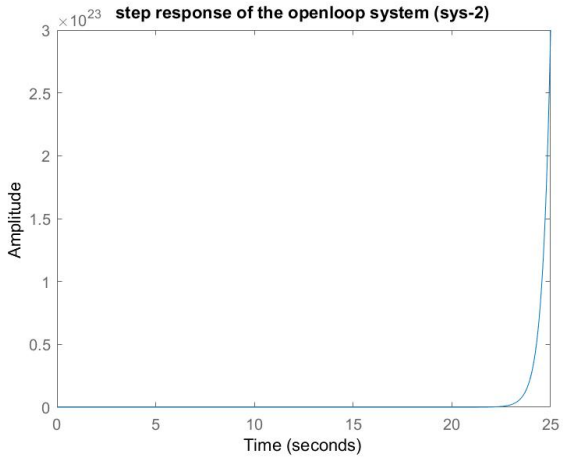

(b)

Figure 4: Open-loop impulse response (a) and step response (b) of **system-2**.

along with the real pole in the right-half plane which gives an exponentially increasing response as a function of time. Similar behaviour can be inferred from the root locus plot of system-1, where again we have an undamped oscillation resulting from imaginary poles.

5.3 PID Controller

5.3.1 System 1 PID

As seen in the above section, open-loop system is highly unstable due to pole in the right half of the s-plane. To make this system stable, the external controller is needed to compensate this unstable pole and move the poles of the system in desired the left half of the s-plane. Before making any progress with controller pole-zero cancellation has been performed for open-

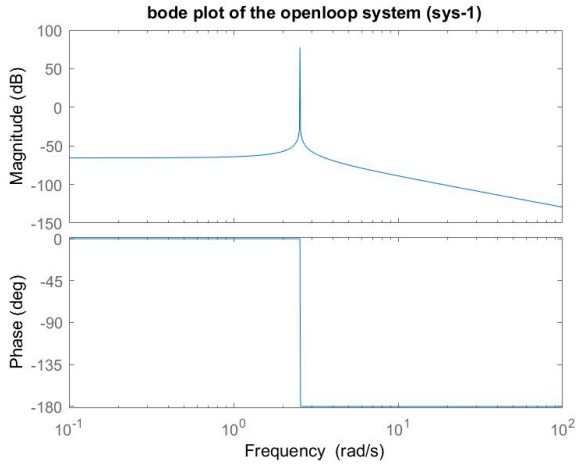

(a)

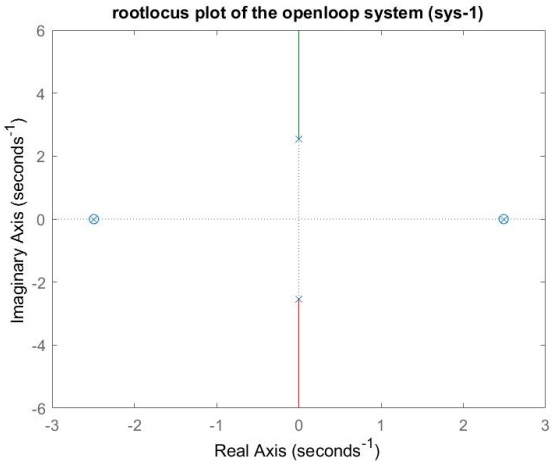

(b)

Figure 5: Uncompensated bode plot (a) and root locus (b) of **system-1**.

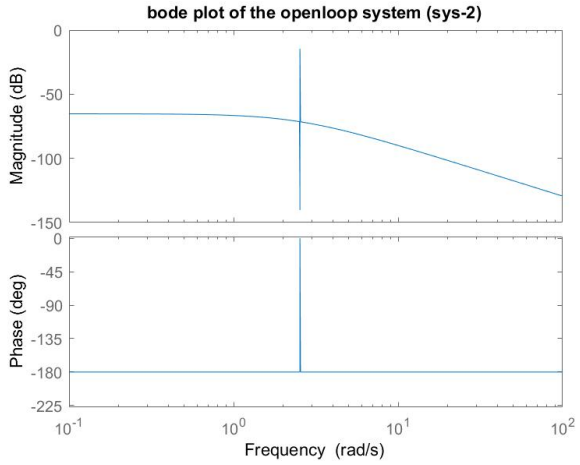

(a)

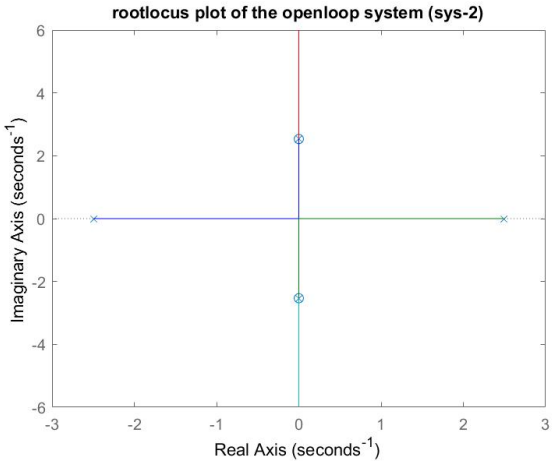

(b)

Figure 6: Uncompensated bode plot (a) and root locus (b) of **system-2**.

loop transfer function to make it a second order system which can be easily controllable by PID controller than fourth order system. After applying the pole-zero cancellation, open-loop transfer function is reduced to Eq. 36,

$$H_1(s) = \frac{0.0033742}{s^2 + 6.414} \tag{36}$$

which gives the transfer function of the PID controller. For tuning the PID gains, `pidtoolbox` was used to obtained optimum values for,

$$\text{PID} = K_p + \frac{K_i}{s} + sK_d. \tag{37}$$

With the values of K_p, K_i, K_d being 2.03e4, 1.77e4, 5.79e3 respectively. The closed-loop system is formed using unit feedback and adding a controller to the system, closed-loop system transfer

function becomes the following,

$$H_{CL,1} = \frac{19.52(s+175)(s+175)}{(s+14.73)(s+3.704)(s+1.096)}. \tag{38}$$

The step response of the closed loop system is given in Fig. 7a, from which it can be seen that the system settles within 3–4 s with roughly 8% overshoot. Furthermore, the response of the closed-loop system to sinusoidal and square waves is given in the Fig. 7b and 7c respectively.

Parameter variation and noise are introduced in the system plant and feedback loop respectively to check the robustness of the design. Plots of comparison of step before and after introducing parameter and noise are given in Fig. 8a and 8b. As can be seen that the designed system is good enough to compensate for small variation and noise in the system and provide reasonably similar step response behavior as a system without them.

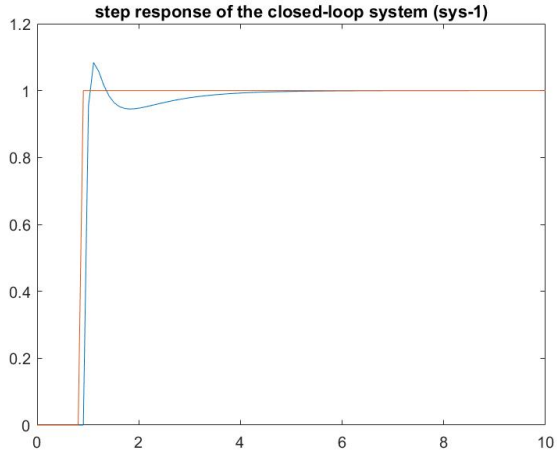

(a)

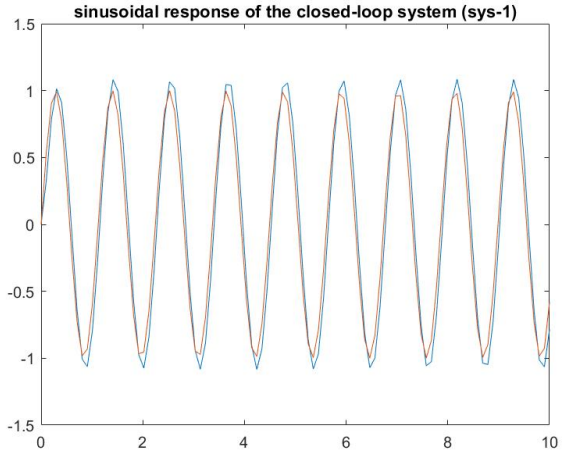

(b)

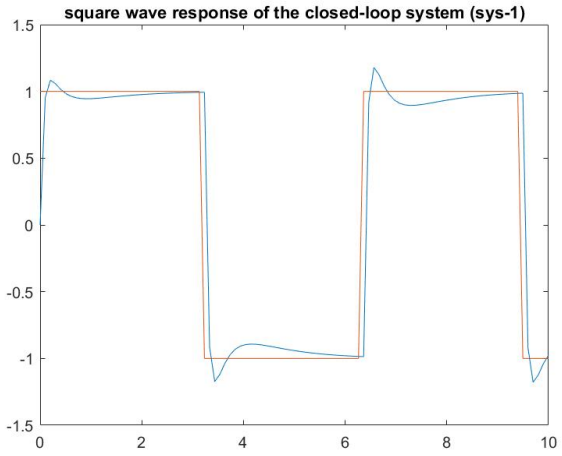

(c)

Figure 7: Closed-loop step response (a), sinusoidal response (b), and square wave response (c) of **system-1** with PID controller. Horizontal axis denotes time, vertical axis amplitude.

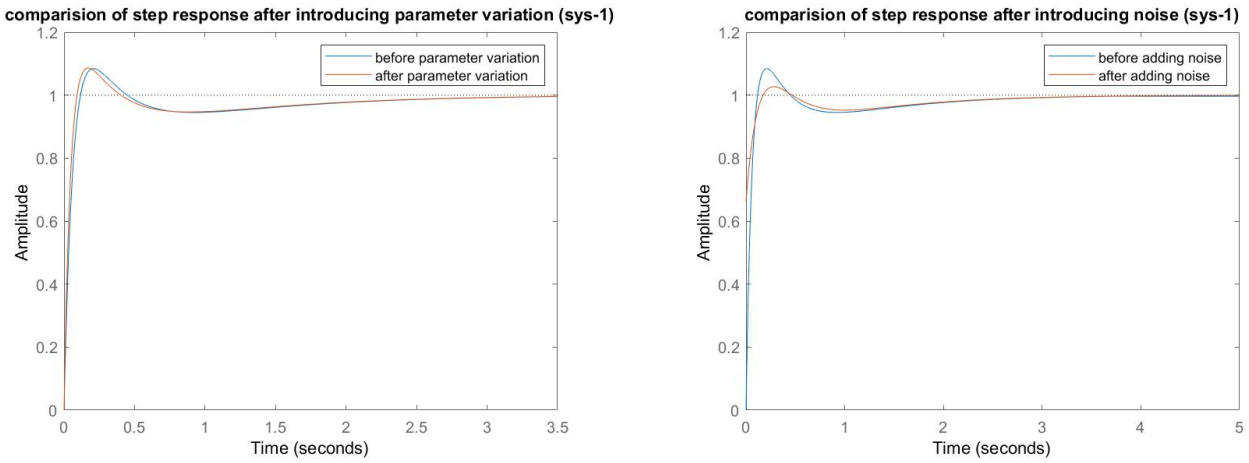

(a) (b)

Figure 8: Effect of parameter variation (a) and noise (b) on the step response of **system-1** with PID controller.

5.3.2 System 2 PID

From the preceeding analysus, it is know that open-loop system 2 is also highly unstable due to pole in the right half of the s-plane. To make this system stable, the external controller is needed to compensate this unstable pole and move the poles of the system in desired the left half of the s-plane. Before making any progress with controller pole-zero cancellation has been performed for open-loop transfer function to make it a second order system which can be easily controllable by PID controller than fourth order system. After applying the pole-zero cancellation, open-loop transfer function is reduced to,

$$H_2(s) = \frac{0.0033742}{(s - 2.491)(s + 2.491)}. \tag{39}$$

Similarly to the process of system-1, `pidtoolbox` was used to retrieve the gains K_p, K_i, K_d with values 2.09e4, 1.83e4, 5.97e3 respectively. Once again we use unit feedback to add a controller to the system, which gives us the closed loop transfer function,

$$H_{CL,2} = \frac{20.156(s + 175)(s + 1.75)}{(s + 16.46)(s^2 + 3.667s + 3.745)}. \tag{40}$$

The step response is given in Fig. 9a, which shows a steeling time of roughly 2–3 s and approximately 14% overshoot. The response of the closed-loop system to sinusoidal and square waves is given in the Fig. 9b and 9c respectively.

Parameter variation and noise are introduced in the system plant and feedback loop respectively to check the robustness of the design. Plots of comparison of step before and after introducing parameter and noise are given in Fig. 10a and 10b. As can be seen that the designed system is good enough to compensate for small variation and noise in the system and provide

reasonably similar step response behavior as a system without them.

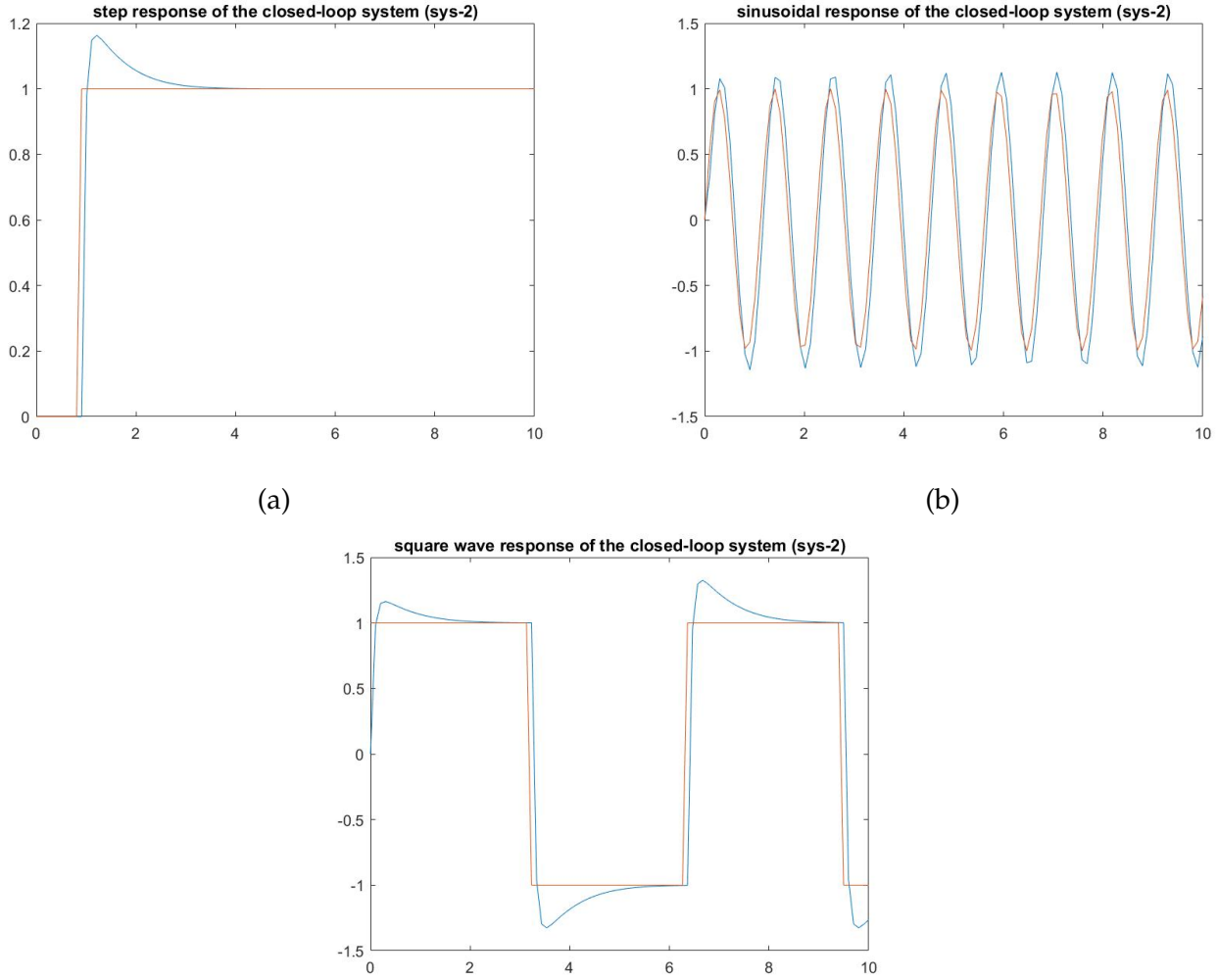

(a) (b)

(c)

Figure 9: Closed-loop step response (a), sinusoidal response (b), and square wave response (c) of **system-2** with PID controller. Horizontal axis denotes time, vertical axis amplitude.

5.4 Full State Feedback Controller

5.4.1 System 1 Full State Feedback

The state space approach is used to design a controller with full state fed back to the system. the control law for this controller is $u = -Kx$. First, the controlabilty of the system is checked and it is found to be completely controllable. Desired poles are placed at 2, -3, -2.5, -3 on the left half of the s-plane. Gains for the controller matrix K are calculated using pole placement methods and are found to be given by

$$K = [1.208e4 \quad 1.604e6 \quad 3.112e3 \quad 6.439e5] \tag{41}$$

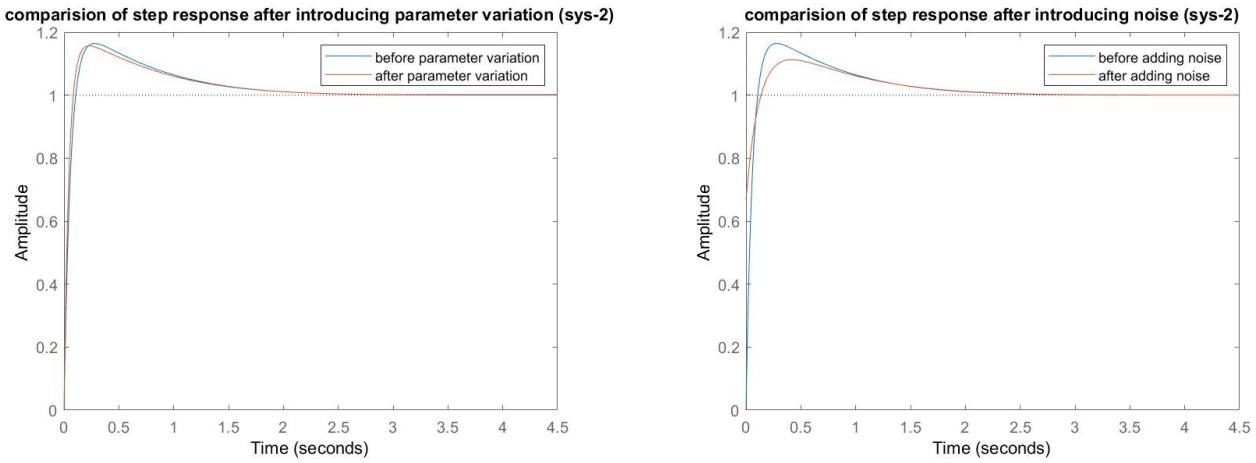

(a) (b)

Figure 10: Effect of parameter variation (a) and noise (b) on the step response of **system-2** with PID controller.

The closed-loop system with full state feedback is given below. Here new closed-loop A is given by $A - BK$ and B is multiplied by scaling factor K_r to account for steady-state error.

$$A = \begin{bmatrix} 0 & 0 & 1 & 0 \\ 0 & 0 & 0 & 1 \\ -47.2 & -5411 & -10.5 & -2172 \\ 0.06243 & 6.203 & 0 & 0 \end{bmatrix} \quad B = \begin{bmatrix} 0 \\ 0 \\ -7.254 \\ 0 \end{bmatrix} \quad C = \begin{bmatrix} 1 & 0 & 0 & 0 \end{bmatrix} \quad D = 0 \tag{42}$$

Step response of the above closed-loop system is given in Fig. 11a. The system takes around 4 seconds to settle without any overshoot. The sinusoidal and square wave response for the closed-loop system is given in the Fig. 11b and 11c.

5.4.2 System 2 Full State Feedback

The approach used to design the K gain matrix shadows exactly that used for system-1. The desired pole locations were select as -2, -3, -2.5, -3 on the left-half of the s-plane. This gave us the gain matrix,

$$K = \begin{bmatrix} -8.394\text{e}5 & 1.208\text{e}4 & 1.496\text{e}4 & 3.112\text{e}3 \end{bmatrix} \tag{43}$$

The closed-loop system with full state feedback is given below. Here new closed-loop A is given by $A - BK$ and B is multiplied by scaling factor K_r to account for steady-state error.

$$A = \begin{bmatrix} 0 & 0 & 1 & 0 \\ 0 & 0 & 0 & 1 \\ -6.414 & 0.06243 & 0 & 0 \\ 2832 & 34.59 & -50.49 & -10.5 \end{bmatrix} \quad B = \begin{bmatrix} 0 \\ 0 \\ 0 \\ 7.016 \end{bmatrix} \quad C = \begin{bmatrix} 0 & 1 & 0 & 0 \end{bmatrix} \quad D = 0 \tag{44}$$

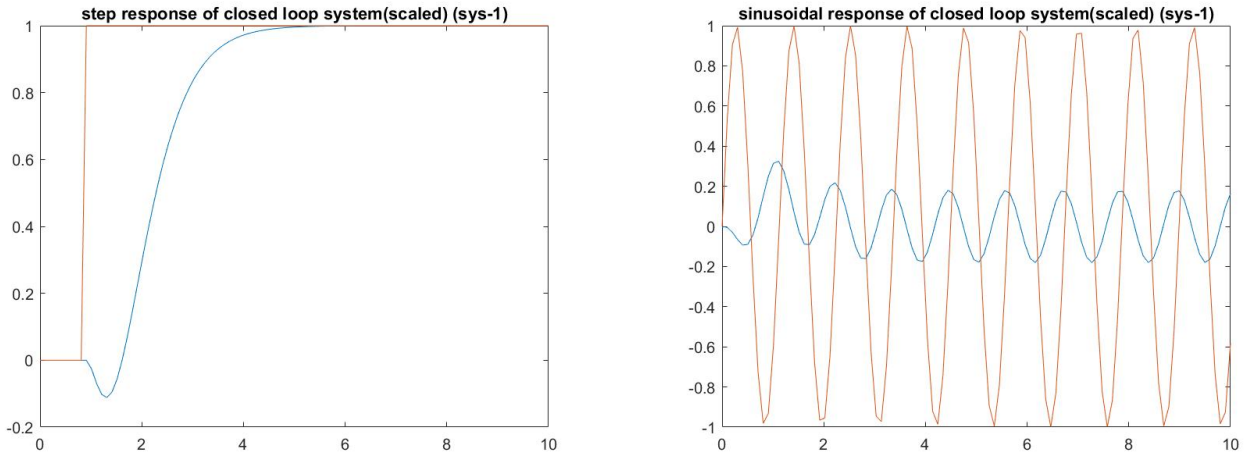

(a) (b)

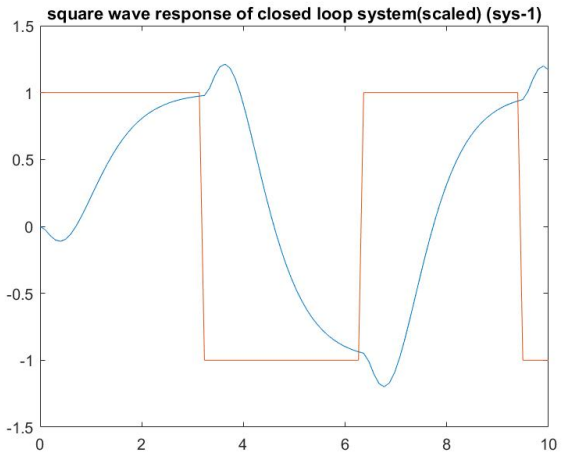

(c)

Figure 11: Closed-loop step response (a), sinusoidal response (b), and square wave response (c) of **system-1** with FSFB controller. Horizontal axis denotes time, vertical axis amplitude.

Step response of the above closed-loop system is given in Fig. 12a. The system takes around 4 seconds to settle without any overshoot. The sinusoidal and square wave response for the closed-loop system is given in the Fig. 12b and 12c.

5.5 Full-order and Reduced-order Observer Design

5.5.1 System 1 Observer Design

First, the full state observer is designed to estimate the states in the feedback. Eq. 45 gives the transfer function of the observer-controller. the transfer function is of 4th order, same as the original system as full state estimator is just a copy of the system. the gains for the observer are found to be $G = \{2.1211e9, 7.8025e8, 3.3068e8, 1.2164e8\}$ for the desired estimator poles {-10, -6, -8, -5}.

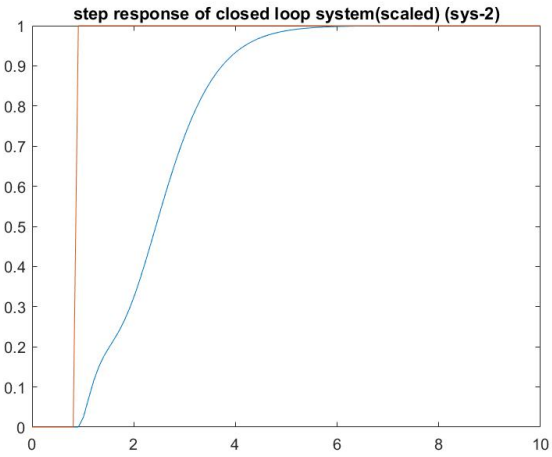

(a)

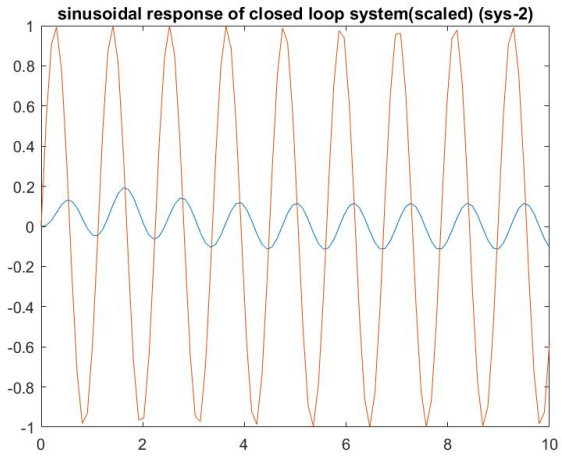

(b)

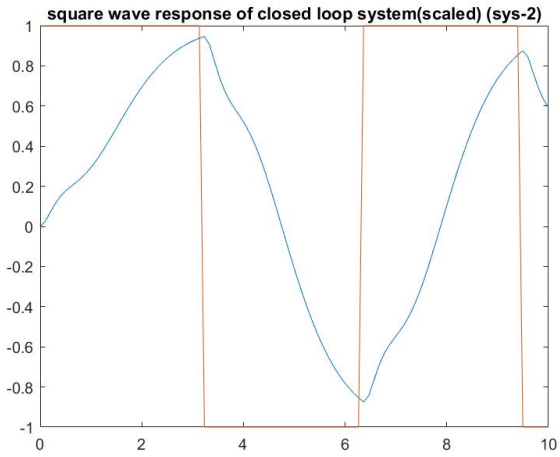

(c)

Figure 12: Closed-loop step response (a), sinusoidal response (b), and square wave response (c) of **system-1** with FSFB controller. Horizontal axis denotes time, vertical axis amplitude.

$$H_{FO,1}(s) = \frac{2.121\text{e}9(s-2.486)(s+2.486)(s+0.1559)}{(s+2.121\text{e}9)(s-2.486)(s+2.486)(s+0.1559)} \tag{45}$$

Step and sinusoidal response of the closed-loop system with full order observer-controller are given in Fig. 13a and 13b respectively.

Reduced-order observer is designed assuming first state y_1 is available for feedback and other states are estimated using the observer. The transfer function for the reduced-order-contoller is given by Eq. 46, which is of 3rd order. Step and sinusoidal response of the closed-loop system with full order observer-controller are given in Fig. 14a and 14b respectively.

$$H_{RO,1}(s) = \frac{1.475\text{e}11(s^2+6.414)(s+2.486)}{(s+2.234\text{e}4)(s-2.228\text{e}4)(s+2.489)} \tag{46}$$

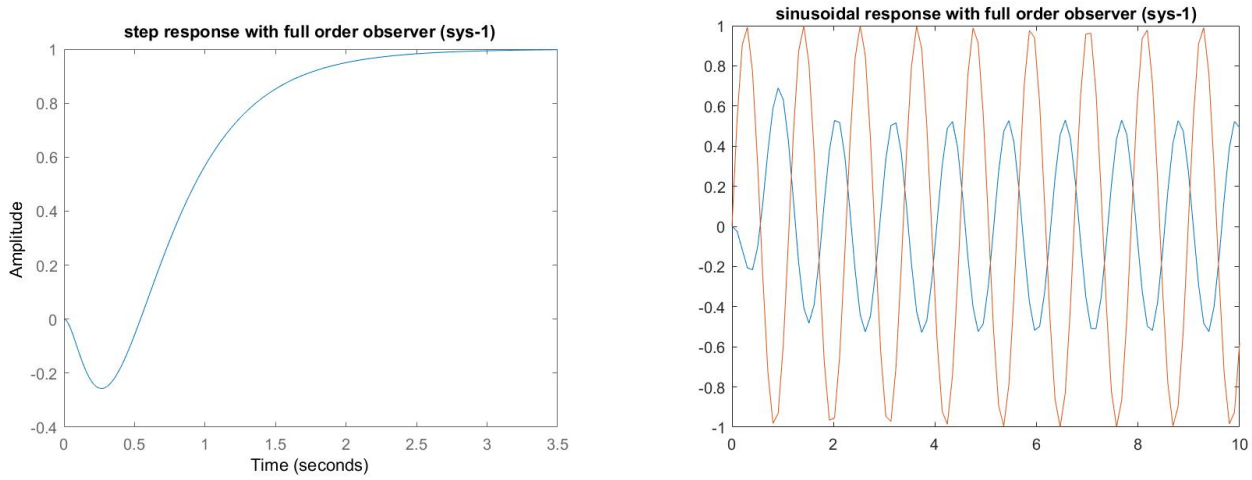

(a) (b)

Figure 13: Step response (a) and sinusoidal response (b) of full order observer-controller for **system-1**.

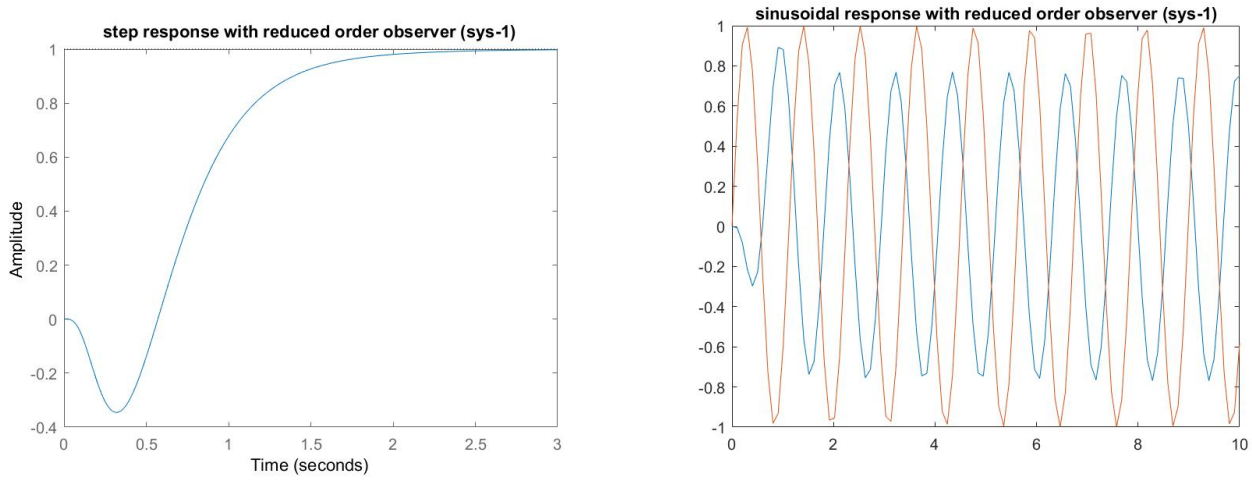

(a) (b)

Figure 14: Step response (a) and sinusoidal response (b) of reduced order observer-controller for **system-1**.

5.5.2 System 2 Observer Design

Similarly as for system-1, the full state observer is designed to estimate the states in the feedback. Eq. 45 gives the transfer function of the observer-controller. The transfer function is of 4th order, same as the original system as full state estimator is just a copy of the system. the gains for the observer are found to be $G = \{9.0491e7, 4.5098e6, -1.4586e7; -7.2648e5\}$ for the desired estimator poles {-5,-2,-3,-1}.

$$H_{FO,1}(s) = \frac{4.510e6(s - 0.161)(s^2 + 7.667)}{(s + 4.510e6)(s - 0.161)(s^2 + 7.667)} \tag{47}$$

Step and sinusoidal response of the closed-loop system with full order observer-controller

are given in Fig. 15a and 15b respectively.

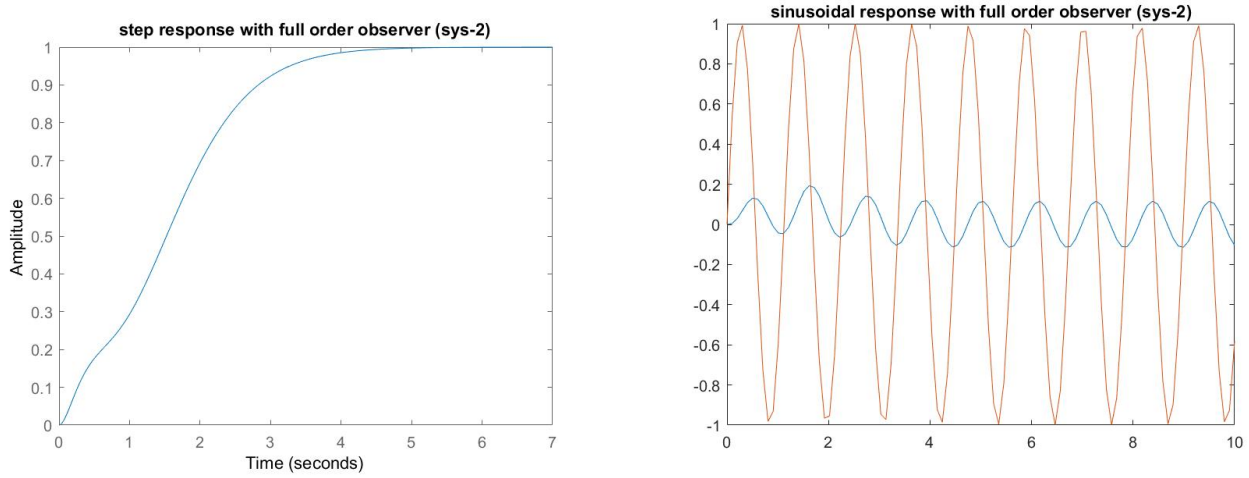

(a) (b)

Figure 15: Step response (a) and sinusoidal response (b) of full order observer-controller for **system-2**.

Once again, the reduced-order observer is designed assuming first state y_1 is available for feedback and other states are estimated using the observer. The transfer function for the reduced-order-contoller is given by Eq. 48, which is of 3rd order. Step and sinusoidal response of the closed-loop system with full order observer-controller are given in Fig. 16a and 16b respectively.

$$H_{RO,2}(s) = \frac{1.135e9(s^2 + 2.582s + 8.505)(s + 2.667)}{(s + 36.16)(s^2 + 28.84s + 743.9)} \tag{48}$$

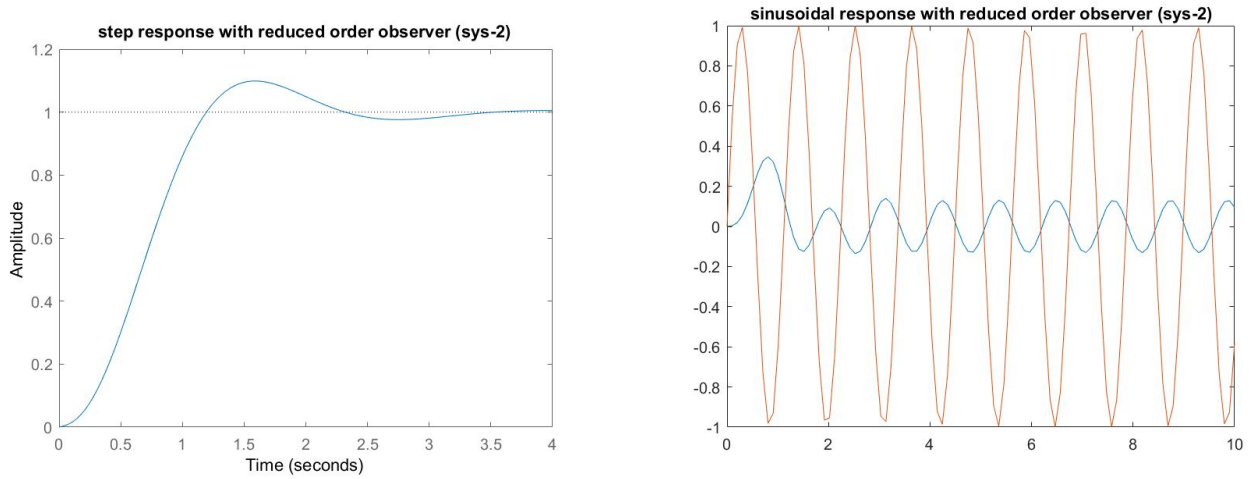

(a) (b)

Figure 16: Step response (a) and sinusoidal response (b) of reduced order observer-controller for **system-1**.

System 1	Specification	PID Controller	FSFB Controller
Delay time	None	0.0331 s	1.37 s
Rise time	< 5	0.0816 s	1.54 s
Peak Overshoot	< 10%	8.41%	0%
Settling time	< 10 s	2.15 s	3.22 s

Table 2: Comparison of results for PID and full state feedback (FSFB) controllers for **system 1**. Settling time is defined for a 2% tolerance from steady state.

System 2	Specification	PID Controller	FSFB Controller
Delay time	None	0.0321 s	1.52 s
Rise time	< 5	0.0772 s	2.56 s
Peak Overshoot	< 10%	16.4%	0%
Settling time	< 10 s	1.68 s	3.82 s

Table 3: Comparison of results for PID and full state feedback (FSFB) controllers for **system 2**. Settling time is defined for a 2% tolerance from steady state.

5.6 Comparison of Step Response Properties

The properties of the step responses of system-1 and system-2 are provided in Tables 2 and 3. Here, the behaviour of these systems when the input is a step is given in terms of (i) delay time, (ii) rise time, (iii) peak overshoot, and (iv) settling time. These properties are contrasted with with respect to the controller used, as well as with respect to the design specifications outlined in Section 3.

6 Discussion

We begin our discussion by recalling the problem statement from Section 2. The primary problem to be solved was whether it is preferable to employ PID or full state feedback to control the position of the magnets. In this section, we discuss the controllers and contrast the advantages and disadvantages of each option. Emphasis will be placed on the metrics outlined in the problem statement to assess the performance of each controller, that is, the ability of the controllers to feasibly meet the design specifications, and the ease of implementation.

Since control design with classical control deals with the transfer function of the system, control design can be performed in both the time and frequency domain. In contrast, in modern control design equations are typically analyzed and implemented in the time domain. We found throughout this project that although classical control is easier to implement, technically

speaking, as most techniques are based on graphical approaches such as root locus or bode plot. However, classical methods are heavily reliant on trial and error to tune the controller (PID in our case). Many well established classical controller designs are based on second-order systems, consequently for higher-order systems, such as those encountered in this report, the concept of dominant poles and pole-zero cancellation is needed to make systems well-behaved. On the other hand, we found that the state-space based pole placement and LQR controller design is provides a more straightforward procedures, especially for higher-order systems, and allows much more control over choosing the desired pole location than classical techniques such as root locus. Another advantage of modern control theory was demonstrated in this project, which is that it can deal with MIMO systems. Contrarily, standard classical control methods can only deal with SISO systems. Despite its limitations, classical control techniques still remained easier to implement, mostly due to the lower amount of mathematics required.

For controlling the unstable open-loop systems, the PID controller caused a considerable amount of headache compared to the modern design. Even with the depth of resources available in MATLAB for designing PID controllers a number of methods were explored, tested, and disregarded as a means of stabilizing the closed loop system. One example is the use of the pidtoolbox, which gave gains on the order of 1e12. Clearly these gains are absurd and would not be feasible to implement in reality. Eventually we chose the cascade the open-loop transfer function with another transfer function that cancels the trouble pole in the right-half plane. This hybrid system was then controlled with a PID. Although this did indeed provide sound results for our simulation, it is noteworthy that pole-zero cancelation of this sort is problematic. For example, uncertainty between the mathematical model and the real system is inevitable, and in this case the cascaded system could become unstable with only minor disturbances. However, for designing the PID controller for the system, it wass necessary to make system second order because tuning a 4th order system was much harder and proved almost impossible with trial and error. Even after all these assumptions, the PID controller holds quite well for some smaller parameter variation and noise in the plant as can be seen in the results in Fig. 8b and 10b.

Contrasting the aforementioned classical method with the full state feedback method, modern control techniques demonstrated to be much more flexible, especially when choosing desired pole locations. Of course this flexibilty came at the cost of increased theoretical complexity. As discussed above, one clear advantage of the full state feedback approach is that for the higher-order system encountered in this project there was no need to reduce the system approximate second-order dynamics as the computations can be performed on the computer. However, with the use of MATLAB these computations are made quite simple and thus most of the mathematical hurdles can be bypassed. Hence, the difficulty of implementing full state feedback is mostly one of conceptual difficulty. Beyond the full state feedback control mechanism, obtaining reliable estimates of the states was discovered in itself to be another technical challenge, one that is not required for classical techniques.

Drawing the reader's attention to Tables 2 and 3, it can be seen that both systems settle to commanded input much faster with the PID controller, roughly twice as fast as the full state

feedback controller. This reduced rise time comes at the cost of a larger overshoot in both of the systems. In contrast, no overshoot was observed with the full state feedback controller. In this way, the step response of the PID controller, being less than a tenth of second, comes off as a sudden jerk in the system. Alternatively, the full state feedback controller has a smoother response which decays to the steady state more gradually. Visualizations of these responses are shown in Fig. 7a, 9a, 11a, and 12a.

7 Conclusion

Upon weighing the advantages and disadvantages of the classical and modern control techniques employed in this report, we have come to the conclusion that modern techniques are unequivocally more robust than classical techniques. This was evidenced by the ad-hoc solution used to control the system with PID. Nonetheless, classical methods have a place, especially when highly accurate and sophisticated control systems are not required. In this case, the complexity of modern techniques may be overkill. With all of the above discussion, the metrics established in Section 3 to assess the different control methods warrant our final decision: full state feedback is the preferable control system for the magnetic levitation system modelled in this report.

References

[1] William L. Brogan. *Modern Control Theory (3rd Ed.)*. Prentice-Hall, Inc., Upper Saddle River, NJ, USA, 1991.

[2] Kash Khorasani. Engr 6131 linear systems lecture notes, December 2019.

[3] Katsuhiko Ogata. *Modern Control Engineering*. Prentice Hall PTR, Upper Saddle River, NJ, USA, 4th edition, 2001.

This concludes the written section.